Photonic crystal waveguide cavity with waist design for efficient trapping and detection of nanoparticles

Pin-Tso Lin, Tsan-Wen Lu, and Po-Tsung Lee*

Department of Photonics and Institute of Electro-Optical Engineering, National Chiao Tung University, Rm. 413 CPT Building, 1001 University Road, Hsinchu 300, Taiwan

potsung@mail.nctu.edu.tw

Abstract: For manipulating nanometric particles, we propose a photonic crystal waveguide cavity design with a waist structure to enhance resonance characteristic of the cavity. For trapping a polystyrene particle of 50 nm radius on the lateral side of the waist, the optical force can reach 2308 pN/W with 24.7% signal transmission. Threshold power of only 0.32 mW is required for stable trapping. The total length of the device is relatively short with only ten photonic crystal periods, and the trapping can occur precisely and only at the waist. The designed cavity can also provide particle detection and surrounding medium sensing using the transmission spectrum with narrow linewidth. The simulated figure of merit of 110.6 is relatively high compared with those obtained from most plasmonic structures for sensing application. We anticipate this design with features of compact, efficient, and versatile in functionality will be beneficial for developing lab-on-chip in the future.

OCIS codes: (230.7380) Waveguides, channeled; (350.4238) Nanophotonics and photonic crystals; (350.4855) Optical tweezers or optical manipulation.

References and links

1. A. Ashkin, "Acceleration and trapping of particles by radiation pressure," Phys. Rev. Lett. **24**(4), 156–159 (1970).
2. A. Ashkin, J. M. Dziedzic, J. E. Bjorkholm, and S. Chu, "Observation of a single-beam gradient force optical trap for dielectric particles," Opt. Lett. **11**(5), 288–290 (1986).
3. R. Omori, T. Kobayashi, and A. Suzuki, "Observation of a single-beam gradient-force optical trap for dielectric particles in air," Opt. Lett. **22**(11), 816–818 (1997).
4. W. H. Wright, G. J. Sonek, and M. W. Berns, "Parametric study of the forces on microspheres held by optical tweezers," Appl. Opt. **33**(9), 1735–1748 (1994).
5. S. Kawata and T. Sugiura, "Movement of micrometer-sized particles in the evanescent field of a laser beam," Opt. Lett. **17**(11), 772–774 (1992).
6. K. Okamoto and S. Kawata, "Radiation force exerted on subwavelength particles near a nanoaperture," Phys. Rev. Lett. **83**(22), 4534–4537 (1999).
7. S. Kawata and T. Tani, "Optically driven Mie particles in an evanescent field along a channeled waveguide," Opt. Lett. **21**(21), 1768–1770 (1996).
8. S. Gaugiran, S. Gétin, J. M. Fedeli, G. Colas, A. Fuchs, F. Chatelain, and J. Dérouard, "Optical manipulation of microparticles and cells on silicon nitride waveguides," Opt. Express **13**(18), 6956–6963 (2005).
9. B. S. Schmidt, A. H. J. Yang, D. Erickson, and M. Lipson, "Optofluidic trapping and transport on solid core waveguides within a microfluidic device," Opt. Express **15**(22), 14322–14334 (2007).
10. A. Rahmani and P. C. Chaumet, "Optical trapping near a photonic crystal," Opt. Express **14**(13), 6353–6358 (2006).
11. M. Barth and O. Benson, "Manipulation of dielectric particles using photonic crystal cavities," Appl. Phys. Lett. **89**(25), 253114 (2006).
12. S. Lin, J. Hu, L. Kimerling, and K. Crozier, "Design of nanoslotted photonic crystal waveguide cavities for single nanoparticle trapping and detection," Opt. Lett. **34**(21), 3451–3453 (2009).
13. O. G. Hellesø, P. Løvhaugen, A. Z. Subramanian, J. S. Wilkinson, and B. S. Ahluwalia, "Surface transport and stable trapping of particles and cells by an optical waveguide loop," Lab Chip **12**(18), 3436–3440 (2012).
14. A. H. J. Yang, T. Lerdsuchatawanich, and D. Erickson, "Forces and transport velocities for a particle in a slot waveguide," Nano Lett. **9**(3), 1182–1188 (2009).

#203510 - $15.00 USD Received 20 Dec 2013; revised 10 Mar 2014; accepted 11 Mar 2014; published 17 Mar 2014

15. A. H. J. Yang, S. D. Moore, B. S. Schmidt, M. Klug, M. Lipson, and D. Erickson, "Optical manipulation of nanoparticles and biomolecules in sub-wavelength slot waveguides," Nature **457**(7225), 71–75 (2009).
16. J. Ma, L. J. Martínez, and M. L. Povinelli, "Optical trapping via guided resonance modes in a slot-Suzuki-phase photonic crystal lattice," Opt. Express **20**(6), 6816–6824 (2012).
17. V. R. Almeida, Q. F. Xu, C. A. Barrios, and M. Lipson, "Guiding and confining light in void nanostructure," Opt. Lett. **29**(11), 1209–1211 (2004).
18. T. Asano, B. S. Song, Y. Akahane, and S. Noda, "Ultrahigh-Q nanocavities in two-dimensional photonic crystal slabs," IEEE J. Sel. Top. Quantum Electron. **12**(6), 1123–1134 (2006).
19. X. Serey, S. Mandal, and D. Erickson, "Comparison of silicon photonic crystal resonator designs for optical trapping of nanomaterials," Nanotechnology **21**(30), 305202 (2010).
20. K. C. Neuman and S. M. Block, "Optical trapping," Rev. Sci. Instrum. **75**(9), 2787–2809 (2004).
21. M. Nieto-Vesperinas, P. C. Chaumet, and A. Rahmani, "Near-field photonic forces," Philos Trans A Math Phys Eng Sci **362**(1817), 719–737 (2004).
22. J. D. Jackson, *Classical Electrodynamics* (John Wiley, 1975), Chap. 6.
23. A. H. J. Yang and D. Erickson, "Stability analysis of optofluidic transport on solid-core waveguiding structures," Nanotechnology **19**(4), 045704 (2008).
24. P. E. Barclay, K. Srinivasan, and O. Painter, "Nonlinear response of silicon photonic crystal microresonators excited via an integrated waveguide and fiber taper," Opt. Express **13**(3), 801–820 (2005).
25. A. E. Cetin and H. Altug, "Fano resonant ring/disk plasmonic nanocavities on conducting substrates for advanced biosensing," ACS Nano **6**(11), 9989–9995 (2012).

1. Introduction

To date, manipulating tiny fragile objects by optical forces with contactless and nondestructive features has inspired many applications ranging from physics to biology. Among these fields, biological particles such as bacteria, proteins, and viruses are always the target to be manipulated. Prior to various configurations, optical tweezers demonstrated by Ashkin *et al.* first utilized highly focused laser beam to perform particle trapping [1]. Near the focus, strong optical forces are established toward point of the highest optical intensity, where particles coming from all directions will be trapped. This technique is regarded useful for handling fragile objects because it can also move the trapped objects with three-dimensional (3D) freedom [2–4]. For trapping particles of size further down to sub-wavelength scale, carefully arranged lens system is always required for better focusing. However, in clinical applications a massive and delicate setup would compromise its utility. Instead, a small and compact system integrated on a chip would be more promising. This unprecedented concept in optical manipulation, later proposed by Kawata *et al.*, is that particles can be trapped or transported by evanescent waves in the near field [5, 6]. By designing structures to well utilize evanescent waves, tiny objects can be manipulated without the massive focusing system. This starts a new branch of integrating particle manipulating system on a chip.

Many on-chip devices, such as optical waveguides [7–9] and cavities [10–12], have been proposed featuring small trapping site approaching nearly the limit of diffraction. Thus the manipulation can be more precise and can handle smaller particles compared to conventional optical tweezers. Among these designs, a waveguide cavity, as proposed by Lin *et al*. [12], shows great potential for manipulation and detection of particles because it incorporates the characteristics of guiding and resonance. Particles attracted onto the waveguide will be transported by the guiding characteristic. When excitation wavelength (λ) matches the cavity resonance, evanescent field enhanced by resonance will stably trap the particles around the cavity. Therefore by tuning the wavelength, we can operate the waveguide cavity with either of the dual modes. Besides, existence of the trapped particle can be detected from shift of the resonant wavelength when the trapping phenomenon occurs. Other than the waveguide cavity, another design using waveguide loop with an intentional gap at the center can also perform both of the dual modes [13]. In which, particles transported along the waveguide will finally be trapped by standing wave in the gap. However, for bending the waveguide to form a loop with negligible loss, the device footprint is inevitably extensive compared to most cavity designs. Besides, the detection function is unachievable for waveguide loop design because the standing wave caused by counter propagating waves brings no spectral information for detection. Therefore, based on the consideration of pursuing compact on-chip devices, resonant trapping structures with additional functionality of detection are more preferable.

#203510 - $15.00 USD Received 20 Dec 2013; revised 10 Mar 2014; accepted 11 Mar 2014; published 17 Mar 2014

In this work, we propose a new waveguide cavity design with waist structure for efficiently trapping and detecting particles of nanometer scale. In most near field configurations, particles are commonly assumed to be trapped on the top of the structures [7–11]. To further exploit optical fields, accessible slot structures are introduced into structure designs as those proposed in refs [11, 12, 14–16]. The slots must be sufficiently small to retain resonant modes while having significant field enhancement inside [17]. But even a small slot can degrade the resonant property of the cavity [12], and it is actually challenging to fabricate such a small slot. Therefore, we intend to trap particles on the side of cavity instead of on the top or in the slot. With both the waist structure and resonant characteristic, optical field distributing around the side of the cavity will be very strong. Accordingly, enhanced optical forces for efficient particle trapping can be achieved. Compared to slot structures, the waist is more accessible for particles because it is open to the surrounding. Thus the size of target particle to be trapped is not limited by the size of slot. Most importantly, the resonant characteristic of the cavity, with proper design, can provide sharp spectral peak for particle detection. For tiny particles, occurrence of the trapping can be known easily by the peak shift of transmission spectrum instead of using a high resolution microscope. These unique properties and benefits of our design are evaluated numerically and compared to reference structures in this study.

2. Structure design

The basic structure of our design is a silicon channel waveguide (refractive index n = 3.46, width w = 500 nm, and height t = 250 nm) with holes (radius r = 150 nm) distributed along longitudinal axis, x, of the waveguide (gray color in Fig. 1(a)). Horizontal plane of z = 0 is set at vertical center of the waveguide. The waveguide is supported on silicon dioxide substrate (n = 1.45) and is assumed to be immersed in water surrounding (n = 1.33) as in real situation for suspending target particles. Distribution of the holes is periodic with period a = 450 nm to form a one-dimensional (1D) photonic crystal lattice. For transverse-electric-like (TE-like) modes with electric field (E) mainly parallel to the xy-plane of the waveguide, this 1D photonic crystal exhibits a photonic band gap (PBG) for wavelength between 1359 nm and 1778 nm (indicated by the shaded range of the black transmission curve in Fig. 1(b)). Waveguide modes in this range are forbidden to transmit through the lattice. The transmission spectrum and the following simulations are all conducted using 3D finite element method (Comsol Multiphysics). A basic cavity is formed by removing single hole as a defect in the lattice. The holes nearest to the defect are shifted outward by a 70 nm displacement (s) to reduce scattering loss of resonance in the cavity [18]. Here we use defect mode instead of widely used localized band edge mode for the following reasons. First, the defect mode has highly concentrated field distribution which is preferable for trapping particle precisely. In the contrary, the localized band edge mode always distributes extensively [19]. Second, optical forces induced by the more concentrated mode will be stronger because of resonant enhancement and its sharp intensity gradient. From the top view (xy-plane at z = 0) and cross-sectional view (yz-plane at x = 0) shown in Fig. 1(c), this basic cavity design already supports a TE-like defect mode with resonant E field on lateral sides of the cavity (indicated by white arrows). However most of the field is well confined in the inaccessible dielectric region. This motivates us to introduce a waist structure to further utilize the resonant field to trap particles. As illustrated by the structure in blue color in Fig. 1(a), two isosceles triangles are carved out from lateral sides of the basic cavity to form the waist which is aligned longitudinally with center of the cavity. We call this design “the waist cavity”. The waist parameters are initially chosen to be 950 nm in length (wl) and 300 nm in width (ww). This cavity design has a resonant peak around 1543 nm within the PBG (shown as the red transmission curve in

#203510 - $15.00 USD Received 20 Dec 2013; revised 10 Mar 2014; accepted 11 Mar 2014; published 17 Mar 2014

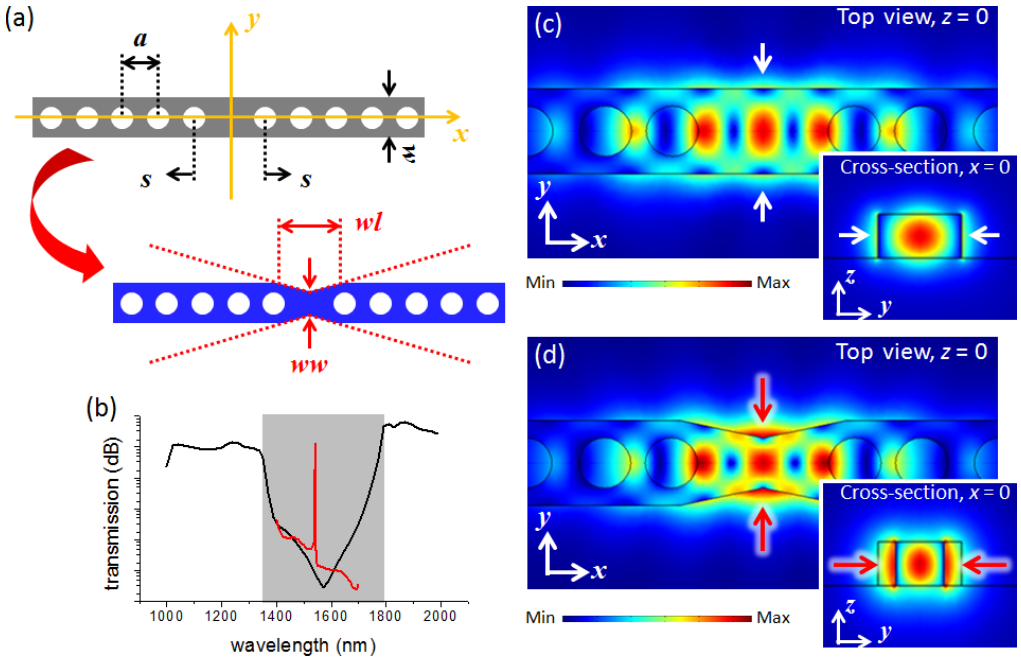

Fig. 1. (a) Schematic illustrations of the basic cavity (gray) and waist cavity (blue) with parameters indicated. (b) Transmission spectra of the designed photonic crystal lattice (black curve) and waist cavity (red curve). The shaded region is the PBG. Top and cross-sectional views of $|E|$ distributions of the resonant modes in (c) the basic cavity and (d) the waist cavity.

Fig. 1(b)). As expected, the induced mode distributes with strong E field extending into water surrounding (indicated by red arrows in Fig. 1(d)). It is worthy to note that the extended field mainly distributes on lateral sides of the waist instead of the top side (cross-sectional view in Fig. 1(d)). This is because the polarization of the mode is mainly parallel to the xy-plane. The continuous boundary condition of normal electric displacement requires drastic rising of E field strength at the lateral sides. With this field distribution, trapping of particle in our design would be very precise, only on lateral sides of the waist. This is an important and unique characteristic for trapping and will be discussed in more detail later.

Figure 2(a) quantitatively shows $|E|^2$ distributions (along y axis) of the resonant modes in the basic and waist cavities when the modes resonate with the same total energy. Comparing with the basic one, field extends more into water surrounding and the intensity is stronger for

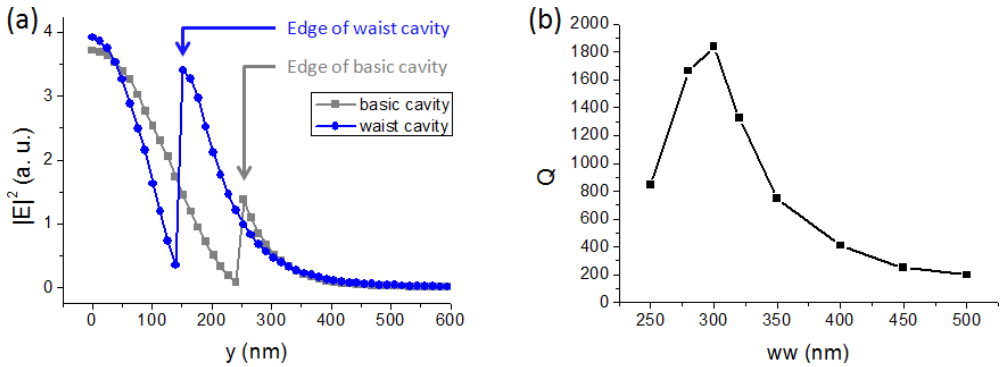

Fig. 2. (a) Distributions of $|E|^2$ of the resonant modes in the basic and waist cavities along y axis when they resonate with the same total energy. (b) Quality factor of the designed waist cavity as a function of ww when s is 70 nm and wl is 950 nm.

#203510 - $15.00 USD Received 20 Dec 2013; revised 10 Mar 2014; accepted 11 Mar 2014; published 17 Mar 2014

the waist cavity. Therefore we can claim that the cavity with waist design has more potential for particle trapping. It is also worthy to note the dependence of quality factor (Q) on the waist width under condition of s = 70 nm and wl = 950 nm with ten periods of holes on both sides of the cavity as shown in Fig. 2(b). Different from the slot structures, the waist design here actually enhances Q of the cavity instead of degrades it. When ww = 300 nm, Q of the resonant mode can reach 1837, which is over nine times enhancement compared with that of the basic cavity without waist (ww = 500 nm).

3. Analysis of particle trapping

To simulate the interaction between particle and resonant field surrounding the waist cavity, we insert a waveguide mode into the structure from one end of the waveguide. The excitation wavelength matches the cavity resonance when particle is presented. Here the particle is assumed to be a polystyrene sphere (PS, n = 1.59 for near infrared) with radius r_p = 50 nm trapped at vertical center of the side of the waist with 20 nm separation between center corner of the waist (CCW) and the PS, that is, centered at x = 0, y = 220 nm, and z = 0. Qs in the following analyses are calculated when the PS is trapped. In many researches, PSs are widely used to represent biological particles because they are similar in optical properties such as absorption and refractive index [14]. Here the PS of 50 nm radius could mimic human immunodeficiency virus (HIV) and rabies virus. Owing to the intermediate particle size, it is not sufficient to treat the PS as either Mie particle (for $r_p >> \lambda$) or Rayleigh particle (for $r_p << \lambda$) [20, 21]. Thus we calculate optical forces on the PS using Maxwell stress tensor without approximation [21–23].

Other than designing a suitable resonant mode, we also need to consider efficient coupling of the input waveguide mode into the cavity resonant mode for efficient particle trapping. Thus we reduce the period number of photonic crystal lattice on the input side of the waveguide while investigating Q and induced trapping force F_y (y component) on the PS, as shown in Fig. 3(a). The force is normalized by input power in unit of pN/W. The negative F_y value implies trapping of particle at positive y side of the waist, and it would be positive if the

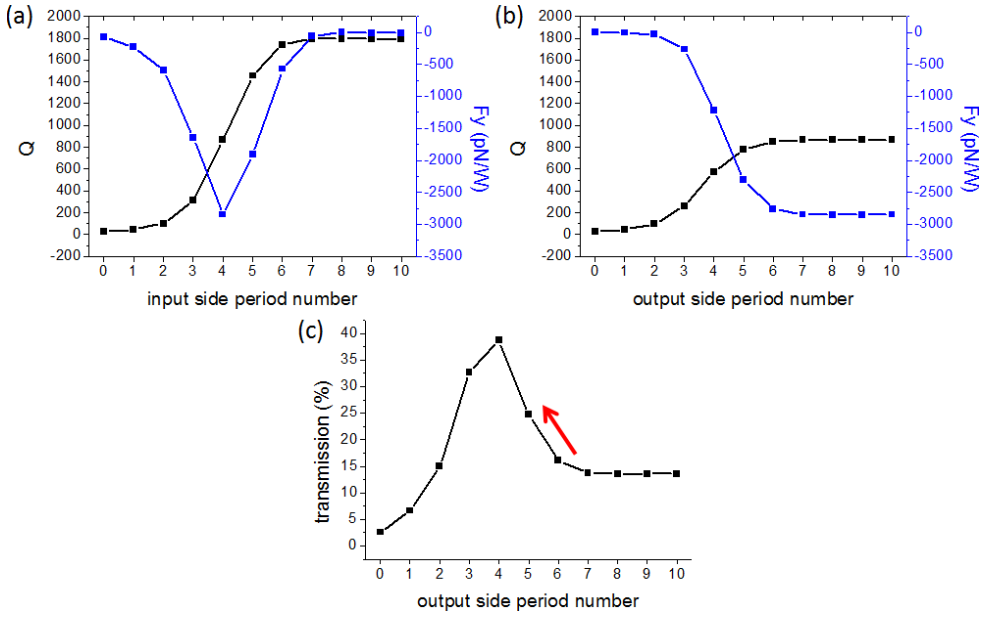

Fig. 3. Dependences of Q and trapping force F_y on the (a) input and (b) output side period numbers. Qs are calculated when the PS is trapped at the side of the waist. (c) Dependence of transmission of the waist cavity on the output side period number when there is only four periods on the input side.

#203510 - $15.00 USD Received 20 Dec 2013; revised 10 Mar 2014; accepted 11 Mar 2014; published 17 Mar 2014

particle is at negative y side of the waist. When the period number is larger than six, enough for the lattice to provide the PBG effect, the cavity can confine the resonant mode well with relatively high Q. But good PBG effect hinders coupling between the waveguide and resonant modes. Hence the optical force induced by the weakly coupled resonance is rather small. When the lattice periods are less than six, Q decreases monotonically as we reduce the period number. This is because the confinement provided by the PBG effect becomes weaker. On the other hand, the waveguide mode can couple into the resonant mode more easily. As a result, the trapping force becomes much stronger. The force reaches its maximum near 2845 pN/W when the input side lattice period number is four. For even fewer periods, the force becomes weak again because the resonant mode can no longer be supported by insufficient PBG effect. Q finally decreases to zero and no resonance can enhance the force. Here we choose four periods on the input side for the strongest trapping force.

As mentioned, the system we want to build is multi-functional. Thus, except trapping ability, spectral information extracted from the device is also important. Here we fix the input side with lattice of four periods and reduce the period number of the output side for better signal transmission. Figure 3(b) shows Q and F_y as functions of lattice periods on the output side. Q and trapping force retain high until six periods. Further reducing the period number makes the PBG effect become weaker and weaker until the resonant mode is no longer supported. Transmission at the waveguide output as we change the period number of the output side is shown in Fig. 3(c). A significant rise in signal transmission is obtained when the lattice period number is reduced from six to five while Q and trapping force only compromise slightly to 782 and 2308 pN/W, respectively. Even so, they are still high enough to provide sharp resonant peak in spectrum and good trapping ability. Hence, we choose five lattice periods on the output side of the waveguide to have both good signal transmission and strong trapping force. Furthermore, the designed waveguide cavity with only ten periods in total is considerably short in length compared with cavity designs utilizing localized band edge modes [19]. This feature of small device footprint meets the goal of developing a compact system. Therefore, in the following investigation the waist cavity is with four and five photonic crystal periods on the input and output sides of the waveguide.

It is important to evaluate how stable the PS can be trapped by the induced optical forces near the structure. Blue curve in Fig. 4(a) shows the evolution of F_y when the PS moves toward the waist along the y axis (x = 0 and z = 0) on resonance. F_y becomes significantly stronger when the PS gets closer and overlaps more with the resonant field. In our simulation, we take 20 nm as the minimum separation between CCW and the PS (centered at x = 0, y = 220 nm, and z = 0) due to the mesh consideration. The exponential evolution implies F_y will be much stronger when the PS gets even closer to the cavity in reality. By integrating parallel component of the force along the path, we can obtain potential energy (U) experienced by the PS. Magenta curve in Fig. 4(a) shows the corresponding potential energy distribution in y

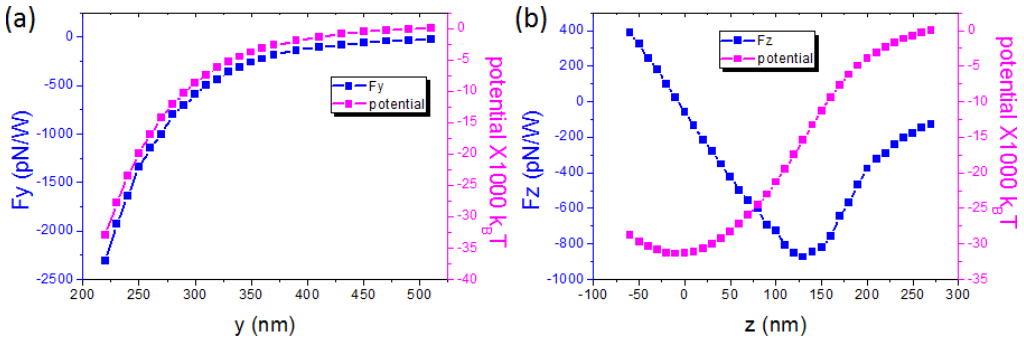

Fig. 4. (a) Evolution of F_y and distribution of trapping potential when the PS moves toward the waist in $-y$ direction (x = 0 and z = 0). (b) Evolution of F_z and distribution of trapping potential when the PS moves toward the waist in $-z$ direction (x = 0 and y = 220 nm). Here T is set at 300K.

#203510 - $15.00 USD Received 20 Dec 2013; revised 10 Mar 2014; accepted 11 Mar 2014; published 17 Mar 2014

direction. A criterion widely used for stable trapping requires depth of the potential energy (ΔU) larger than $10kBT$ [2, 11, 12], where k_B is the Boltzmann constant and T is the system temperature. Here we set T as room temperature 300K. In Fig. 4(a), ΔU of $32913k_BT$ is much deeper than the requirement, and it could be even deeper when the PS approaches further closer to CCW. This result manifests the trapping ability of the waist cavity. Curves in Fig. 4(b) show the trapping characteristic of the resonant mode when the PS moves toward the cavity along vertical path with $x = 0$ and $y = 220$ nm (in $-z$ direction). The z component of the trapping force (F_z) evolves from negative value to positive value when the PS crosses the plane of $z = 0$. This evolution resembles that of the restoring force of a spring system. The equilibrium point at $z = 0$ corresponds to the deepest point of potential energy distribution in z direction. Again, the depth of $31332k_BT$ is much deeper than $10k_BT$. The threshold power for stable trapping is only 0.32 mW. This value is relatively small compared to many prior designs [12, 13]. Therefore, our design certainly can be regarded as an efficient trapping system. Besides, the corresponding total energy stored in the waist cavity under the threshold input power is only 0.1 fJ, which is much lower than the energy for the cavity investigated in ref [24] occurring nonlinear effects.

After confirmation of the excellent trapping ability of our cavity design, we continue to investigate whether the PS would be trapped elsewhere to claim precise trapping at the waist. From Fig. 1(d), we observe that the field around the nearest holes is also strong. To achieve the feature of precise trapping, the induced forces should not be able to pull the PS into these holes. Thus we check the force when the PS (centered at $x = -440$ nm, $y = 0$, and $z = 195$ nm) is at entrance of the hole as indicated by position a. in Fig. 5. At this position, F_z on the PS is −347 pN/W. When the trapping force at the waist just satisfies the requirement of stable trapping (under threshold power excitation), the corresponding F_z at the hole entrance is merely −0.11 pN. This is rather weak compared with the force F_y of −0.74 pN at the waist. The PS perturbed by Brownian motion will easily pass these holes instead of being pulled into them. We also check the force when the PS (centered at $x = 0$, $y = 0$, and $z = 195$ nm) is above top center of the cavity as indicated by position b. in Fig. 5. This is to confirm that the particle will only be trapped on the lateral sides of the waist instead of the top surface. At this position, F_z on the PS is −430 pN/W. It would be as weak as −0.14 pN under threshold power excitation (0.32 mW). Again, the PS perturbed by Brownian motion will easily pass this site. Finally the PS will only be stably trapped on the lateral sides of the waist as indicated by position c. in Fig. 5. Hence, we can conclude that our proposed trapping design can definitely realize precise trapping. This comparison is summarized in Table 1.

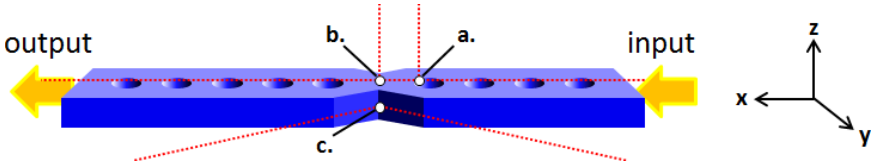

Fig. 5. Schematic illustration of the designed waist cavity with three possible trapping positions indicated. The positions are at entrance of the nearest hole (position a.), on top center (position b.), or at the lateral side of the waist (position c.).

Table 1. Comparison of trapping forces on the PS when it is at different positions.

position	a.	b.	c.
Coordinate	(−440 nm, 0, 195 nm)	(0, 0, 195 nm)	(0, 220 nm, 0)
Trapping force	$F_z = -347$ pN/W	$F_z = -430$ pN/W	$F_y = -2308$ pN/W
Trapping force under threshold power excitation	−0.11 pN	−0.14 pN	−0.74 pN

#203510 - $15.00 USD Received 20 Dec 2013; revised 10 Mar 2014; accepted 11 Mar 2014; published 17 Mar 2014

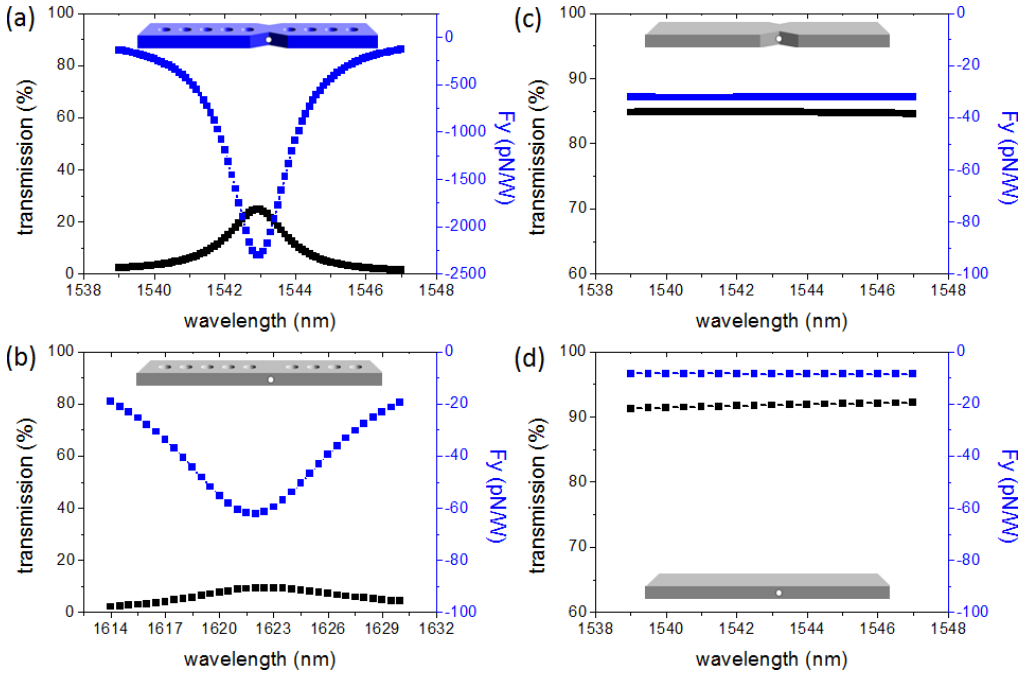

Fig. 6. Spectra of transmission and trapping force F_y on the PS when it is trapped on the lateral side of (a) the waist of the designed cavity, (b) the basic cavity without the waist, (c) the waist of a ridge waveguide, and (d) a ridge waveguide. In each of these cases, the PS is at position $x = z = 0$ and a 20 nm separation between the particle and CCW or edge of the waveguide.

To stress the merits provided by introducing the waist structure, we compare the trapping ability of the designed waist cavity with several reference structures and discuss the spectral information offered. Figure 6(a) shows spectra of the trapping force (F_y) and transmission when the PS (centered at $x = 0$, $y = 220$ nm, and $z = 0$) is trapped on the lateral side of the waist of the designed cavity. Since only one resonant mode exists in the PBG, we observe only one peak enhanced by the resonance. The peak values of F_y and transmission are –2308 pN/W and 24.7% respectively around wavelength of 1543 nm. Linewidth of the transmission peak is 1.7 nm (fitted by Lorentz function), corresponding to Q of 782. Here a narrow linewidth is preferable because it provides fine spectral resolution for particle detection. Figure 6(b) shows spectra of another case when the PS (centered at $x = 0$, $y = 320$ nm, and $z = 0$) is trapped on the lateral side of the basic cavity (without the waist). Here the basic cavity is also with four and five photonic crystal periods on the input and output sides of the waveguide. Both F_y and transmission are enhanced by the resonance of the corresponding cavity mode. But the peak of F_y is only –62 pN/W because less field of the resonant mode extends to interact with the PS compared with that of the designed waist cavity. Meanwhile, the transmission peak drops to 9.3% with linewidth broadened to be 13.1 nm and Q reduced to be only 150. Subsequently, we remove the holes and investigate the spectra when the PS is trapped by a ridge waveguide with or without the waist at positions indicated in Figs. 6(c) and 6(d). In the case with the waist, the PS (centered at $x = 0$, $y = 220$ nm, and $z = 0$) is trapped on the lateral side of the waist. And in the case without the waist, the PS (centered at $x = 0$, $y = 320$ nm, and $z = 0$) is just trapped on the sidewall of the ridge waveguide. Because there is no confinement provided by the photonic crystal along x direction to support a resonance, the spectra are nearly constant. Therefore, they bring no spectral information for particle detection even though the transmissions are high in both cases. Compared with the case without the waist, F_y on the PS at the waist is stronger because there is more extended field at the waist for interacting with the PS. Nevertheless, these forces are actually considerably small compared to that induced by the resonant mode of the designed waist cavity. Moreover,

#203510 - $15.00 USD Received 20 Dec 2013; revised 10 Mar 2014; accepted 11 Mar 2014; published 17 Mar 2014

the waist reflects and scatters the guided mode in the ridge waveguide, which leads to lower transmission for the ridge waveguide with the waist. From these comparisons, we again demonstrate that our cavity design with the waist structure is very promising for particle trapping. Besides, the sharp peak provided in transmission spectrum would be very helpful for particle detection, as discussed in the following.

So far, we show that the PS as small as 50 nm in radius can be stably and precisely trapped by our cavity design at the waist. But to visually observe the trapping phenomenon is very difficult because the PS is too small to see even using a microscope of high magnification. A better and promising way to detect nano-particle trapping is through the transmission spectrum. Figure 7(a) shows the transmission spectra before and after the PS of 50 nm radius is trapped by the waist cavity. The transmission spectra after trapping a PS of 75 or 100 nm radius are also provided. Each of these trapped PSs is on the lateral side of the waist of the designed cavity, centered at $x = 0$, $z = 0$, and a 20 nm separation between CCW and the particle. Trapping of the PS with 50 nm radius causes a 0.5 nm red-shift in peak wavelength. The shift is small but still clearly detectable attributed to the narrow linewidth. For larger PS, the peak wavelength shifts more. With these as database, we cannot only detect trapping of particle but also recognize the size of the trapped particle by the amount of peak shift.

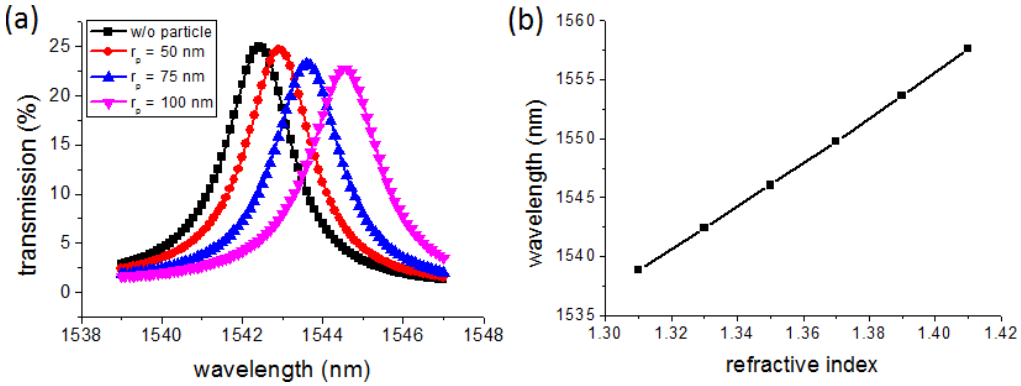

Fig. 7. (a) Transmission spectra of the designed waist cavity when no particle is trapped and when a PS of 50, 75, or 100 nm radius is trapped. (b) Resonant wavelength of the transmission peak as a function of refractive index of the surrounding medium.

Other than particle detection, the designed waist cavity can be applied to sense the surrounding medium by analyzing the peak wavelength of the transmission spectrum. Figure 7(b) shows the relation between the refractive index of the surrounding medium and the corresponding resonant wavelength of the transmission peak. Slope of the curve represents the sensitivity of our design in unit of nm/RIU, where RIU is the refractive index unit. The calculated value is 188.0 nm/RIU and the corresponding figure of merit (FOM), defined as sensitivity divided by spectral linewidth, is 110.6, which is relatively high compared with those obtained from most plasmonic structures for sensing application [25]. In addition to precise trapping ability under low power consumption, we show that our cavity design also possesses excellent detection and sensing capabilities, which meets the goal of developing a compact device with versatile functionalities.

4. Summary

We propose a photonic crystal waveguide cavity design with a waist structure for trapping particles in the near field region on a chip. By introducing the waist structure with $ww = 300$ nm and $wl = 950$ nm, the resonance characteristic of the cavity mode can be enhanced with Q rising from 198 to 1837 while there are ten photonic crystal periods on both input and output sides of the waveguide. For efficient coupling into the cavity mode resonance and extracting transmission signal, we reduce the input and output side lattices to four and five periods

#203510 - $15.00 USD Received 20 Dec 2013; revised 10 Mar 2014; accepted 11 Mar 2014; published 17 Mar 2014

respectively. Although this lattice reduction will sacrifice resonance characteristic, the resulted Q of 782 is still sufficiently high to provide enhancement on the trapping force (F_y) and the device length is relatively short with only ten periods in total. For trapping a PS of 50 nm radius on the lateral side of the waist, the force can be enhanced to 2308 pN/W with 24.7% signal transmission. The investigation of trapping potential shows that a threshold power of only 0.32 mW is required for stable trapping, and the trapping occurs precisely and only on the lateral sides of the waist. A narrow linewidth of 1.7 nm can resolve small shift of resonant peak caused by trapping a particle of various sizes. Even the PS of 50 nm radius, which is too small to be observed from an imaging system, can be detected. The designed waist cavity can also provide the function of surrounding medium sensing. The calculated FOM of 110.6 is relatively high compared with those obtained from most plasmonic structures for sensing application. Therefore, we can conclude that our waist cavity design with precise trapping on the lateral sides of the waist, detection, and sensing capabilities is compact, efficient, and versatile in functionality.

Acknowledgments

This work is supported by Taiwan's National Science Council (NSC) under contract numbers NSC-100-2221-E-009-109-MY3 and NSC-101-2221-E-009-054-MY2.

#203510 - $15.00 USD Received 20 Dec 2013; revised 10 Mar 2014; accepted 11 Mar 2014; published 17 Mar 2014